# CONDITIONS OF PASSAGE AND ENTRAPMENT OF TERRESTRIAL PLANETS IN SPIN-ORBIT RESONANCES

Valeri V. Makarov
United States Naval Observatory, 3450 Massachusetts Ave. NW, Washington DC, 20392-5420, USA; vvm@usno.navy.mil

## ABSTRACT

The dynamical evolution of terrestrial planets resembling Mercury in the vicinity of spin-orbit resonances is investigated using comprehensive harmonic expansions of the tidal torque taking into account the frequency-dependent quality factors and Love numbers. The torque equations are integrated numerically with a small step in time, including the oscillating triaxial torque components but neglecting the layered structure of the planet and assuming a zero obliquity. We find that a Mercury-like planet with a current value of orbital eccentricity (0.2056) is always captured in 3:2 resonance. The probability of capture in the higher 2:1 resonance is approximately 0.23. These results are confirmed by a semi-analytical estimation of capture probabilities as functions of eccentricity for both prograde and retrograde evolutions of spin rate. As follows from analysis of equilibrium torques, entrapment in 3:2 resonance is inevitable at eccentricities between 0.2 and 0.41. Considering the phase space parameters at the times of periastron, the range of spin rates and phase angles for which an immediate resonance passage is triggered is very narrow, and yet a planet like Mercury rarely fails to align itself into this state of unstable equilibrium before it traverses 2:1 resonance.

*Key words:* celestial mechanics – planets and satellites: dynamical evolution and stability – planet–star interactions

*Online-only material:* color figures

## 1. INTRODUCTION

Planets of terrestrial type with solid mantles are subject to triaxial and tidal torques exerted by their host star. A planet just formed from the protoplanetary disk rotates at a much higher rate than the rate of its orbital motion. In the course of millions to billions of years, the secular terms of the tidal torque cause the planet to spin down. The tidal bulges moving across the planet at different frequencies result in a gradual loss of kinetic energy through friction and heating. The energy dissipation rate is normally so slow that most of the major planets in the solar system still rotate faster than they revolve around the Sun, with the exception of Venus with its slow retrograde rotation and Mercury, which is in a 3:2 spin-orbit resonance (Pettengill & Dyce 1965). Presumably, the planet traversed a number of higher-order resonances before it reached this state. The ultimate, and the most stable, state for a rotating planet subject to tidal forces is 1:1 resonance, when the rotation rate is equal to the orbital rate, and the planet is always pointing with its most elongated dimension toward the star. The dissipation of the energy of rotation also diminishes the obliquity of the planet's equator, gradually aligning the axes of rotation and of the orbit. Mercury's dynamical evolution has been much faster than that of other solar planets, because (1) it is closer to the Sun and (2) its orbital eccentricity varied in a relatively wide range and has been higher than the eccentricity of the other close-in planets. The importance of eccentricity for Mercury's chaotic evolution was emphasized by Correia & Laskar (2004, 2009), who upwardly revised the original estimate of the probability of capture to the present 3:2 resonance at 7% (Goldreich & Peale 1966).

Mercury can serve as a good model for smaller-mass, rocky exoplanets, especially those orbiting M dwarfs in their habitable zones. Although the exact rheology of exoplanets will remain a matter of speculation for the foreseeable future, it seems reasonable to adopt the parameters and models obtained for the Earth and the Moon. The objective of this paper is to investigate the circumstances of the transition of a Mercury-like planet with an Earth-like rheology through a high-order spin-orbit resonance. In this case, the widely accepted approximations for the value of tidal torque in the vicinity of a resonance are not applicable. Furthermore, the oscillatory terms of the force cannot be neglected. We employ high-order expansions of the torque in harmonics of tidal frequency and powers of eccentricity, and a relation for the Love number as a function of tidal frequency in terms of real and imaginary compliances (Section 2). The resulting differential equation of second order, which includes both the tidal and triaxial torque components, is integrated with a step much smaller than the period of rotation, with the current best estimates for Mercury (Section 3). With the current value of eccentricity ($e = 0.20563$), the planet traverses 2:1 resonance with an estimated probability of 0.77, and is always captured in 3:2 resonance. The transition is very fast, accompanied by a significant step-down in the average rotation rate. In Section 4, more integrations are performed with the initial rate set to exactly a 2:1 resonance and with various initial phase angles. It is revealed that such a planet inserted in resonance almost always stays in it. The actual passage through resonance can only occur through a tiny area of the phase space around a phase angle of $+\pi/2$ or $-\pi/2$. A qualitative physical explanation for this curious fact is given. We discuss in the final Section 5 why our model planet is unlikely to traverse 2:1 resonance despite the tightness of the required conditions to do so. We derive the probabilities of capture in spin-orbit resonances for both prograde and retrograde evolutions of spin rate, and compare them with the ranges of equilibrium eccentricities.

## 2. HARMONIC EXPANSIONS OF TORQUES

The instantaneous torque acting on a rotating planet is the sum of the triaxial torque, caused by the quadrupole

**Table 1**
Explanation of Notations

| Notation | Description |
| --- | --- |
| $\xi$ | Moment of inertia coefficient |
| $R$ | Radius of planet |
| $T$ | Torque |
| $M_2$ | Mass of planet |
| $M_1$ | Mass of star |
| $a$ | Semimajor axis of planet |
| $r$ | Instantaneous distance of planet from star |
| $v$ | True anomaly of planet |
| $e$ | Orbital eccentricity |
| $M$ | Mean anomaly of planet |
| $B$ | Second moment of inertia |
| $A$ | Third moment of inertia |
| $C$ | Moment of inertia around spin axis |
| $n$ | Mean motion, i.e., $2\pi/P_{orb}$ |
| $\mathcal{G}$ | Gravitational constant, $= 66468$ m$^3$ kg$^{-1}$ yr$^{-2}$ |
| $\tau_M$ | Maxwell time, i.e., ratio of viscosity to unrelaxed rigidity[a] |
| $\mu$ | Unrelaxed rigidity modulus |
| $\alpha$ | Tidal lag responsivity |

**Note.** [a] For the differences between relaxed and unrelaxed rigidity moduli, see Efroimsky (2012a, 2012b).

inertial momentum, and the tidal torque, caused by the dynamic deformation of its body. In neglect of the obliquity (Danby 1962),

$$\ddot{\theta} = \frac{T_{TRI} + T_{TIDE}}{\xi M_2 R^2} \qquad (1)$$

with $\theta$ being the sidereal angle of the planet reckoned from the axis of its largest elongation. All other notations used in this formula and throughout the paper are explained in Table 1. We consider the specific but representative case when the obliquity of the planet's equator is small ($i \simeq 0$) and the planet is not too close to the star ($R/a \ll 1$). Neglecting the precession and nutation of the planet, the triaxial torque is (Danby 1962; Goldreich & Peale 1966)

$$T_{TRI} = -\frac{3}{2}(B - A)n^2\frac{a^3}{r^3}\sin 2(\theta - v). \qquad (2)$$

Using the comprehensive development of Kaula and Darwin's harmonic decomposition of the tidal torque by Efroimsky & Lainey (2007), Efroimsky & Williams (2009), and Efroimsky (2012a, 2012b), one can write a simplified equation for the tidal torque, which we call Efroimsky's torque

$$\begin{aligned}
T_{TIDE} = \frac{3}{2}\mathcal{G}M_1^2\frac{R^5}{a^6}\sum_{q=-1}^{4} G_{20q}(e)\sum_{j=-1}^{4} G_{20j}(e) \\
\times [K_c(2, \chi_{220q})\,\text{Sign}(\omega_{220q})\cos((q-j)M) \\
+ K_s(2, \chi_{220q})\sin((q-j)M)],
\end{aligned} \qquad (3)$$

where the positively defined forcing frequency

$$\chi_{220q} = |\omega_{220q}| = |(2 + q)n - 2\dot{\theta}|, \qquad (4)$$

the so-called $G$-functions of Kaula $G_{20j}$ are related to power series in eccentricity via Hansen's coefficients (e.g., Dobrovolskis 1995):

$$G_{20j}(e) = X_{2+j}^{-3\ 2}(e), \qquad (5)$$

and the all-important "quality functions" are

$$K_c(l, \chi) = -\frac{3}{2(l-1)}\frac{\Lambda_l \chi \Im(\chi)}{(\Re(\chi) + \Lambda_l\chi)^2 + \Im^2(\chi)} \qquad (6)$$

$$K_s(l, \chi) = \frac{3}{2(l-1)}\frac{\Re^2(\chi) + \Im^2(\chi) + \Lambda_l\chi\Re(\chi)}{(\Re(\chi) + \Lambda_l\chi)^2 + \Im^2(\chi)}. \qquad (7)$$

Finally, the remaining terms in this equation are

$$\Lambda_l = \frac{4\pi(2l^2 + 4l + 3)R^4\mu}{3l\mathcal{G}M_2^2}, \qquad (8)$$

and

$$\begin{aligned}
\Re(\chi) &= \chi + \chi^{1-\alpha}\tau_A^{-\alpha}\cos\left(\frac{\alpha\pi}{2}\right)\Gamma(1+\alpha) \\
\Im(\chi) &= -\tau_M^{-1} - \chi^{1-\alpha}\tau_A^{-\alpha}\sin\left(\frac{\alpha\pi}{2}\right)\Gamma(1+\alpha).
\end{aligned} \qquad (9)$$

The $\Re(\chi)$ and $\Im(\chi)$ functions are the real and imaginary parts of the complex compliance, respectively. Equation (3) includes oscillating terms of the tidal torque, $q \neq j$. For a planet similar to Mercury, these oscillating terms prove very small and can be safely neglected.[1] The results of integration over 20,000 years were hardly different with or without these terms. Omitting the oscillating terms of the tidal torque, we arrive at the simplified expression for the secular part of the torque

$$T_{TIDE} = \frac{3}{2}\mathcal{G}M_1^2\frac{R^5}{a^6}\sum_{q=-1}^{4} G_{20q}^2(e)K_c(2, \chi_{220q})\,\text{Sign}(\omega_{220q}). \qquad (10)$$

Note that expansions (3) and (10) are limited to $l = 2$. The higher-order expansion terms ($l = 3$) are neglected because the coefficients are at least eight orders of magnitude smaller than the $l = 2$ terms for Mercury or similar planets. The expansion in harmonics of mean anomaly is limited to the range $q, j = -1, 0, \ldots, 4$ for the ease of computation, the other terms being much smaller than these six. For example, $G_{205}(0.20563) = 0.019$, to be compared with $G_{200}(0.20563) = 0.896$, and the rest of the Kaula coefficients for the omitted terms are even smaller. The crucial differences between this approach and the previous studies, e.g., by Celletti et al. (2007), is that more realistic relations are employed here for the "quality functions" of tidal frequency (Equations (6) and (7)) with rheological parameters supported by observations and theory, and that full account is taken of the fast, oscillating terms of the triaxial torque, which are integrated in a small step.

## 3. INTEGRATION OF MERCURY

The evolution of Mercury's spin can be considered as a template model of a rocky, relatively small planet whose eccentricity can be driven to sufficiently large values due to the interactions with larger planets in the system. It is also one of the few planets whose physical parameters are fairly well known (Anderson et al. 1987). The parameters used in our computations are listed in Table 2. The Maxwell time $\tau_M$ was set to Earth's value, assuming a similar composition and temperature. The sensitivity of this crucial parameter to temperature has to be

---

[1] The oscillating components of the tidal torque cannot be neglected for a nearly spherical planet, i.e., when $(B - A)/C$ is very small.
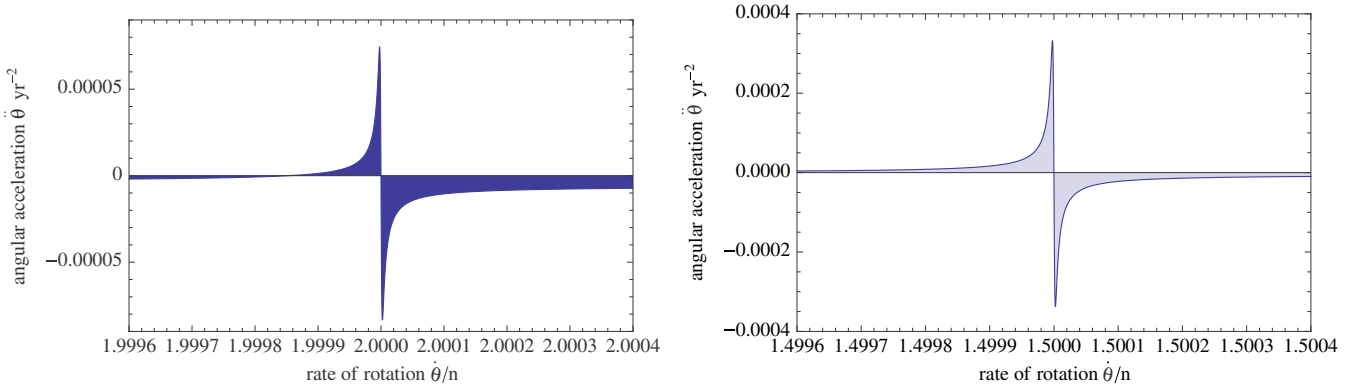
**Figure 1.** Rotation acceleration caused by the secular tidal torque (i.e., $j = q$ in Equation (3), or Equation (10)) on a Mercury-like planet in the vicinity of 2:1 resonance (left) and 3:2 resonance (right). Dramatic variations of the torque are confined to very narrow ranges of frequencies, while the effective torque integrated over a wider range of frequencies is negative. The variable, antisymmetric part of the torque is caused by the given resonance. The almost constant negative offset is due to the contribution of other resonances. Despite their appearance on the chosen scale, the functions are smooth and differentiable.

(A color version of this figure is available in the online journal.)

**Table 2**
Parameters of the Mercury Integration

| Parameter | Value |
|---|---|
| $\xi$ | $\frac{2}{5}$ |
| $R$ | $2.44 \times 10^6$ m |
| $M_2$ | $3.3 \times 10^{23}$ kg |
| $M_1$ | $1.99 \times 10^{30}$ kg |
| $a$ | $5.79 \times 10^{10}$ m |
| $e$ | $0.20563$ |
| $(B - A)/C$ | $1.2 \times 10^{-4}$ |
| $n$ | $26.088$ yr$^{-1}$ |
| $\tau_M$ | $500$ yr |
| $\mu$ | $0.8 \times 10^{11}$ kg m$^{-1}$ s$^{-2}$ |
| $\alpha$ | $0.2$ |

taken into account for rocky exoplanets whose interiors may be significantly hotter. Higher temperatures result in smaller viscosity and, thus, much shorter Maxwell times. The rigidity $\mu$ was also set to the value for the Earth. The characteristic time $\tau_A$ is in fact frequency-dependent, and we modeled it as

$$\tau_A(\chi) = 50000 \exp(-\chi/0.2) + 500 \qquad (11)$$

in years. This expression is chosen to represent the expected behavior of $\tau_A$, which sharply rises toward small frequencies. However, the results proved quite insensitive to the functional form of $\tau_A$. In fact, practically the same conclusions can be obtained by simply setting $\tau_A = \tau_M$. Again, this may not be the case for hotter, less viscous planets.

The tidal torque at a given eccentricity is a slowly varying function of spin rate everywhere except the vicinity of spin-orbit resonances $\dot\theta = (1 + q/2)n$. Figure 1 shows in detail the dependence of the overall angular acceleration $\ddot\theta$ of the planet caused by the secular tidal torque only, in the vicinity of 2:1 ($q = 2$) and 3:2 ($q = 1$) resonances. Note that the dramatic changes of tidal torque take place within a very narrow interval of tidal frequencies. The widely used assumption that $\ddot\theta \propto -\dot\theta$ is justified only in a vanishingly small range of spin rates, i.e., $\dot\theta \in [1.9999977, 2.0000023]n$ in the case of 2:1 resonance and for the chosen value of the Maxwell time $\tau_M$. The amplitude of the oscillatory triaxial torques outside the 1:1 resonance is a few orders of magnitude greater than the peak values of the tidal torque (Figure 2). The scale of free librations, caused by the triaxial torque, is also a few orders of magnitude greater than
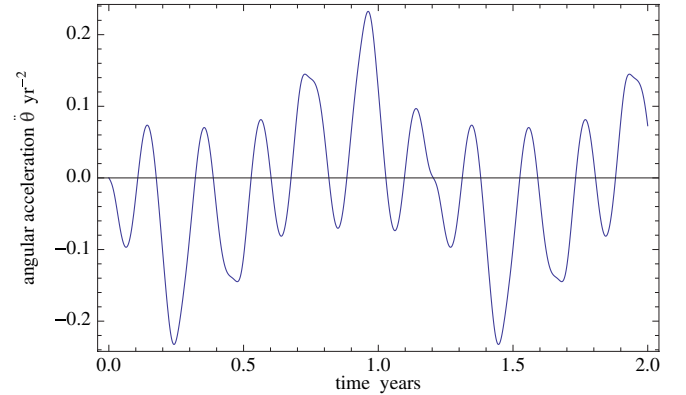


**Figure 2.** Rotation acceleration caused by the triaxial torque on a Mercury-like planet as a function of time at $\dot\theta = 1.6\,n$.

(A color version of this figure is available in the online journal.)

the characteristic width of the kink in Figure 1. The net effect of the secular tidal force integrated over one libration period is to spin the planet down. This follows from the fact that the mean value of acceleration at $\dot\theta = 2n$ integrated over a much wider interval than the width of the kink, is negative for these resonances. The peak torque below the resonance rate tapers off quickly and becomes negative at $\dot\theta = 1.999895\,n$. The torque function near 3:2 resonance (Figure 1, right) is similar in shape, but the amplitude is larger and the positive shoulder below the resonance is much broader. The 1:1 resonance is fundamentally different from the higher-order counterparts in that the tidal torque is positive at all rotation rates between 0 and $n$.

### 3.1. Probabilities of Capture in 2:1 and 3:2 Resonances

The ordinary differential equation (1) was integrated with a grid of initial conditions $\theta(0)$, $\dot\theta(0)$ for 30,000–55,000 years with a maximum step of $2 \times 10^{-3}$ yr. The initial mean anomaly was always set to $M(0) = 0$. For 2:1 resonance, a grid of 40 integrations with $\dot\theta(0) = 2.013\,n$ and $\theta(0) = \pi i/40$, $i = 0, 1, \dots, 39$ was performed. These integrations resulted in 9 captures and 31 passages of the resonance. Therefore, the estimated probability of 2:1 capture is 0.23 at the current value of eccentricity. The amplitude of free libration gradually increases as the planet spins down toward the point of resonance. Once a lower swing in $\dot\theta$ reaches the resonance, a fast transition into a

new spin state occurs on a timescale of a few years. The average rate takes a sudden leap to a significantly smaller value, and the libration starts to decrease. This set of simulations shows that the chance of Mercury being captured into the 2:1 resonance at the current value of eccentricity is modest.

The outcome of integrations in the vicinity of 3:2 resonance is quite different. A similar set of integrations with $\dot{\theta}(0) = 1.518\,n$ and $\theta(0) = \pi\,i/40, i = 0, 1, \ldots, 39$ resulted in 40 captures. The estimated probability of 3:2 capture is 1. As soon as $\dot{\theta}$ reaches the point of resonance, the amplitude of libration abruptly doubles, but the mean rotation stays around $1.5\,n$. Once the planet is captured, the amplitude of libration starts to slowly decline. The period of libration starts to decrease immediately after the capture. A longer integration for 100,000 yr shows that the period of libration asymptotically approaches 16 yr, which is the theoretical value (Murray & Dermott 2000) for the physical parameters listed in Table 2. This confirms the validity of our computations of the triaxial torque. Further numerical experiments revealed that the planet traverses 3:2 resonance in a similar manner to 2:1 resonance at significantly smaller values of eccentricity. We conclude that our numerical simulations are consistent with the fact that Mercury is entrapped in a 3:2 resonance with the current value of eccentricity. This outcome is indeed most likely unless the eccentricity acquired much different values in the past. An even higher eccentricity would have resulted in entrapment in a 2:1 resonance long in the past when the planet was approaching this rotation rate. Alternatively, a considerably smaller eccentricity at the moment of approaching 3:2 resonance would have made the planet traverse it quickly and continue to spin down.

### 3.2. Equilibrium Torques and Evolution of Eccentricity

Correia & Laskar (2004) pointed out that Mercury's eccentricity has varied chaotically during its long dynamical evolution in the solar system. The current state of Mercury, entrapped in a 3:2 spin-orbit resonance, is the result of a long history of tidal and orbital interactions, probably marked by multiple passages of spin-orbit resonances. In particular, if the initial spin rate of Mercury was much greater than it is today, the planet has successfully traversed a number of higher resonances. Understanding the dependence of tidal torque on eccentricity in the framework of Efroimsky's model is as important as the truthful estimation of capture probabilities in each resonance.

Correia & Laskar (2004, 2009) employed a linear torque model, also known as MacDonald's torques (Goldreich & Peale 1966) or the Constant Phase Lag model (Ferraz-Mello et al. 2008), in which the secular torque is linearly dependent on the time derivative of tidal frequency. As we noted in Section 3, Efroimsky's torque is linear only in vanishingly narrow intervals around resonances (Figures 1(a) and (b)). The widely used assumption that the secular tidal torque is linear everywhere across the range of relative spin rates $\dot{\theta}/n$ leads to well-known problems and inconsistencies. For example, a slowing down Moon in the absence of quadrupole momentum is not allowed to descend into 1:1 resonance (synchronous rotation) for any nonzero eccentricity (Murray & Dermott 2000; Williams & Efroimsky 2012), because the linear torque, monotonously increasing with growing eccentricity, changes sign from negative to positive at a certain equilibrium eccentricity for any fixed $\dot{\theta}/n > 1$. Therefore, a perfectly spherical Moon should have stalled in its de-spinning at a higher than synchronous rate, namely, $\dot{\theta}_{\text{equ}}/n = 1 + 6e^2 = 1.018$. This is not the case for Efroimsky's tidal torque, which sharply
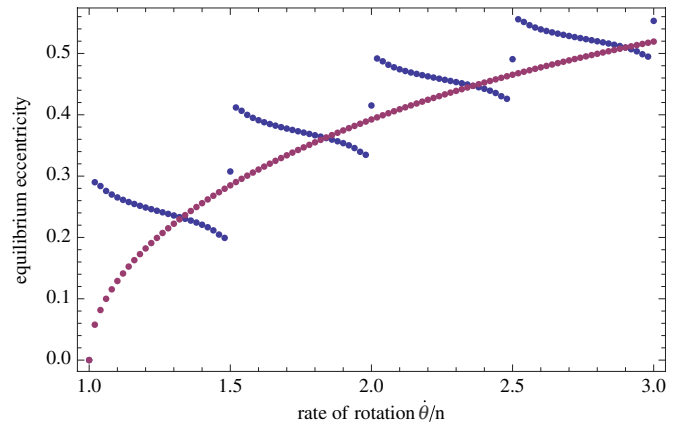


**Figure 3.** Equilibrium eccentricity of a Mercury-like planet separating the areas of negative (spin-down) and positive (spin-up) secular tidal torque for a grid of relative rates of rotation. The smooth curve represents the linear torque widely used in the literature. The jagged curve represents Efroimsky's torque.

(A color version of this figure is available in the online journal.)

decreases at supersynchronous rotation rates, counteracting the effects of eccentric motion. The dependence of equilibrium eccentricity, whence the linear torque disappears, for a range of rotation rates is depicted in Figure 3 with the monotonously rising dotted line. It implies that synchronous rotation, so commonly observed among the satellites of the solar system, is not attainable for any nonzero eccentricity. If Mercury traversed 3:2 resonance and continued to spin down toward synchronization, it would be stuck at an equilibrium rate of $1.24\,n$ with the current value of eccentricity.

The character of equilibrium torques is profoundly different with Efroimsky's model, depicted with the jagged dotted curve in Figure 3. The curve was obtained by finding the roots of Equation (10) in $e$ for a grid of $\dot{\theta}/n$. The grid resolution is chosen such that only the slow variations of the equilibrium eccentricity outside the resonances are faithfully represented. The first jump from $e_{\text{equ}} = 0$ at $\dot{\theta}/n = 1$ to $e_{\text{equ}} \approx 0.29$ just slightly above the synchronous rate implies that Mercury is allowed to be captured in 1:1 resonance if the eccentricity is not too large ($e < 0.29$), evolving either from slower or faster rotation rates. Likewise, entrapment in 3:2 resonance is inevitable for $0.2 < e < 0.41$ if Mercury reaches this rate of rotation from either direction. This is consistent with the results of numerical simulations in Section 3.1 that the probability of 3:2 capture with the current value of eccentricity is 1. What happens if Mercury reaches $\dot{\theta}/n = 1.5$ with an eccentricity below 0.2? Capture is still possible, but the probability declines with decreasing eccentricity (see Section 5). Entrapment of the planet in 2:1 resonance is inevitable for $0.34 < e < 0.49$, etc. The teeth of the equilibrium torque curve act as very efficient resonance traps for a planet like Mercury, whose eccentricity varies in a fairly wide range over billions of years of dynamical evolution.

## 4. CONDITIONS OF TRAVERSING A RESONANCE

The purpose of our next set of simulations is to find out under which circumstances the planet traverses a spin-orbit resonance. We have established that the test planet passes the point $\dot{\theta} = 2\,n$ quite quickly, within several years. At some moment during this passage, the planet is at periastron with a rotation rate close to $2\,n$. What is the rotation angle $\theta$ at this time, and does this value matter for the way this dynamical transformation unfolds? One
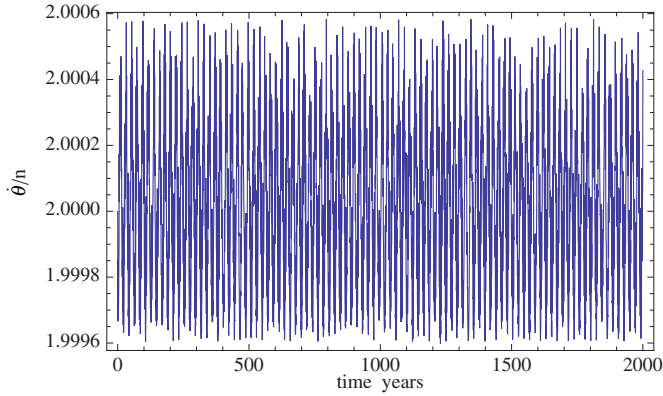
**Figure 4.** Results of integration of the Mercury-like test planet with initial conditions of resonance, $\dot\theta(0) = 2n$, $\theta(0) = 0$. The spin rate remains in resonance with the orbital motion indefinitely long.

(A color version of this figure is available in the online journal.)



**Figure 5.** Similar to Figure 4, but with a different initial phase angle, $\theta(0) = \pi/2$. The planet traverses the resonance after a couple of libration oscillations, in less than 100 yr.

(A color version of this figure is available in the online journal.)

hundred integrations were conducted with the planet initially already at resonance spin rate ($\dot\theta(0) = 2n$), but with initial phase angles ranging from $-\pi/2$ to $+\pi/2$ in equal steps. For most of the interval of possible initial angles, the planet is clearly captured in resonance, i.e., the spin rate continues to oscillate around the resonant value. A typical example of such entrapment with the initial conditions $\dot\theta(0) = 2n$, $\theta(0) = 0$, is shown in Figure 4. The rate of rotation oscillates around the resonant point roughly between $1.9996\,n$ and $2.0006\,n$, seemingly forever. The oscillations (not resolved in the figure) are distinctly non-sinusoidal immediately after the capture. The amplitude of these oscillations slowly declines with time. The tidal bulge still runs across the circumference of the planet with a period equal to the orbital period; therefore, the tidal dissipation of energy goes on. A slow shrinkage of the orbit is the main source of tidal energy for a planet captured in spin-orbit resonance.

The result is drastically different if we set the initial conditions to $\dot\theta(0) = 2n$, $\theta(0) = \pi/2$ (Figure 5). After a couple of upward swings, the spin rate jumps through the resonance point in $\sim 80$ years. The spin rate resets abruptly at considerably lower mean values. The peak rates never quite reach the resonance value, gradually diminishing with time. A sidereal angle $\theta = \pm\pi/2$ at $M = 0$ implies that the planet is positioned sidewise with respect to the star, that is, its longer dimension is perpendicular to the Sun–planet line. This is the preferred configuration, which is necessary for the planet to traverse resonance. The range of suitable phase angles at $\dot\theta(0) = 2n$ and $M(0) = 0$, which make it possible for the planet to traverse the resonance, is quite small, approximately between $\pi/2 - 0.030$ and $\pi/2 + 0.021$. Remarkably, at any other $\theta(0)$ in $[0, \pi]$, the planet remains entrapped in this resonance. Thus, the passage through resonance cannot occur unless the planet is turned almost sidewise with respect to the star at one of the periastrons. A stronger tidal dissipation during the last circulation before resonance would not allow the planet to reach this range, and capture becomes inevitable.

Such strong requirements for the orientation of the planet at the point of resonance may seem puzzling at first glance. However, simple qualitative considerations of the interaction of the tidal and triaxial torques explain the matter. Let us consider a triaxial planet in a resonance $2\dot\theta = (2+q)n$, so that for each of the two orbital revolutions, it makes exactly $2+q$ rotations about its axis. Assume $\theta(0) = 0$ at an initial periastron passage, so that the longest dimension is aligned with the instantaneous direction
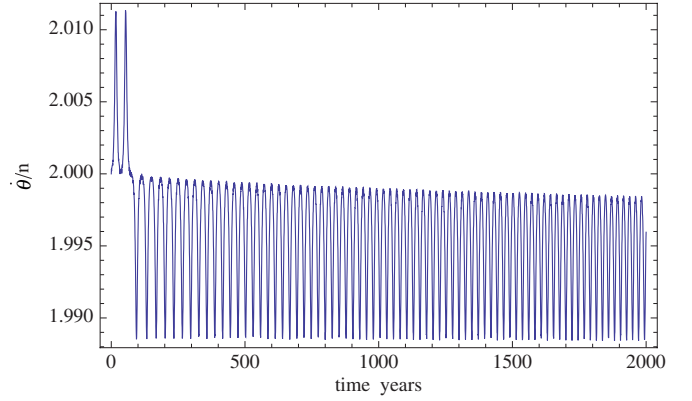
to the star. After two complete orbital revolutions, the planet arrives at periastron with a slight lag in phase angle because the tidal torque decelerated the planet's rotation. The planet therefore is tilted opposite from the spin direction. The triaxial torque will act to re-align the planet again, so that the average action from the triaxial torque is to spin up the planet again. This counteraction of the triaxial torque is symmetric, in that if the planet's spin accelerated during the two complete orbits the torque will rectify its rotation. Thus, any deviation of spin rate from the resonance value will be automatically corrected by the triaxial torque. The planet is trapped in a stable equilibrium. This is not the case when the initial angle at periastron is $\pm\pi/2$. Any net lag in phase angle will cause a nonzero triaxial torque in the same direction, causing the planet to continue to spin down. In this configuration of unstable equilibrium, the torque assists the tides to swiftly turn the planet around and lunge through the resonance.

The same mechanics work for a circular orbit ($e = 0$). One may ask then, how a planet initially at $\theta(0) = 0$ can be entrapped at all, if at some point afterward it inevitably turns sidewise with respect to the star? The answer is that while the planet turns through $\pi/2$ with respect to the star, the spin rate will change because of the triaxial torque, and will no longer be equal to $(1 + q/2)n$. In other words, the condition of resonance passage is a certain area of the two-dimensional phase space.[2] Returning to Figure 5, we note that the point of the phase space $\{\theta(0) = \pi/2, \dot\theta(0) = 2n\}$ does not actually belong to this area, because the passage through resonance is not immediate. Indeed, the planet has to realign its phase space parameters in two upward swings before it traverses the resonance at about 80 yr after the start of integration. In order to map the phase space of *immediate* resonance passages, we performed several hundred short-term integrations (for 1000 yr) varying the initial $\dot\theta(0)$ with a step of $5 \times 10^{-5}n$ and $\theta(0)$ with a step of $1 \times 10^{-5}$ rad. The mapped section of this space for our Mercury-like planet and 2:1 resonance is shown in Figure 6 as a green-shaded area. If the planet at periastron turns up within the green area, it immediately traverses resonance. This "green corridor" is extremely narrow in $\theta$ at $\dot\theta/n > 2$ and occupies a tiny fraction of the phase space. The black dots display the periastron positions of the planet. The dots are lined up in five consecutive libration trajectories,

---

[2] In fact, the relevant phase space is three-dimensional if we include the initial mean anomaly $M(0)$, but for simplicity of analysis, we restricted our study to the plane $\{\theta, \dot\theta\}$ by considering only the instances of periastron.
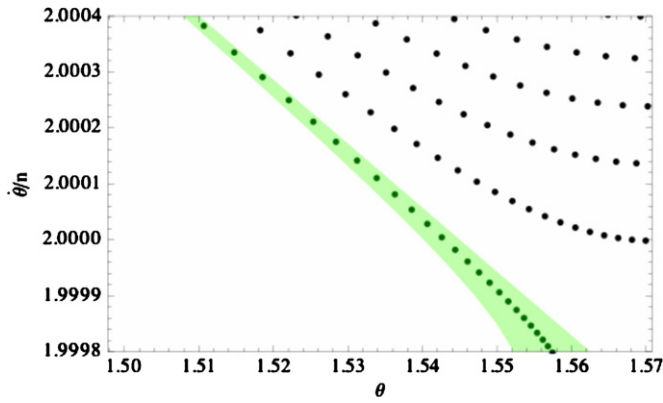
**Figure 6.** Small section of the $\{\theta, \dot{\theta}\}$ phase space around the 2:1 spin-orbit resonance. The green-shaded area is the subspace of initial parameters from which a direct passage through resonance takes place. The dots show consecutive periastron positions of the test planet. Parts of four libration swings gradually approaching the point of resonance are visible before the final trajectory hits the passage area and follows it through resonance into the domain of lower spin rates, $\dot{\theta} < 2n$.

(A color version of this figure is available in the online journal.)

each following one probing lower spin rates around $\theta = \pi/2$. The final lap hits the "needle's eye" and falls through resonance, never to return to it. Note that the next to last trajectory actually reached $\dot{\theta} = 2n$ at $\theta$ very close to $\pi/2$, but the tipping point is at a slightly smaller $\theta$.

## 5. DISCUSSION

The area of the phase space above the resonant spin rate, through which a Mercury-like planet can traverse a resonance, is very narrow. For example, the appropriate phase angle at periastron for $\dot{\theta} = 2n$ should be between $\pi/2 - 0.03065$ and $\pi/2 - 0.02575$. It may appear improbable that the planet, driven by the relatively large triaxial torques, and wandering through a good part of the phase space in its pre-resonance evolution, can hit this very small passage opening. And yet, as we established through many numerical integrations, the test planet in most cases passes resonances higher than 3:2, if the integration starts well above the resonant spin rate. The camel rarely fails to go through this needle's eye.

In the domain of above-resonance spin rates, the passage area extends almost along a straight line toward higher $\dot{\theta}/n$ and smaller $\theta$. Figure 6 shows only a segment of this area. The needle's eye area looks more like a needle, stretching out to at least $\theta = \pi/2 - 0.9031$, $\dot{\theta}/n = 2.009$, tapering off to a point. On the other hand, the lower extents of libration swings tend to probe the area of unstable equilibrium, i.e., the minimum point of each trajectory is close to $\theta = \pi/2$. This important fact follows from the integral of energy for free librations in the vicinity of a resonance $q$ averaged over one orbital period (Murray & Dermott 2000), which can be written as

$$\frac{1}{4}C\dot{\gamma}^2 - \frac{3}{2}n^2(B-A)G_{20q}(e)\cos(\gamma) = E_0, \qquad (12)$$

where $\gamma = 2\theta - (2+q)M$ and $E_0$ is a constant energy. When the rate of rotation is still faster than the resonant value, $2\dot{\theta} > (2+q)n$, but it is at the minimum of a libration swing, $\dot{\theta} = \min$, the cosine in this equation should be equal to $-1$, hence, $\gamma = \pi$. At the times of periastron, the corresponding value of $\theta$ is $\pi/2$. Figures 7(a) and (b) show larger parts of the phase space in the vicinity of a 2:1 resonance passage and a
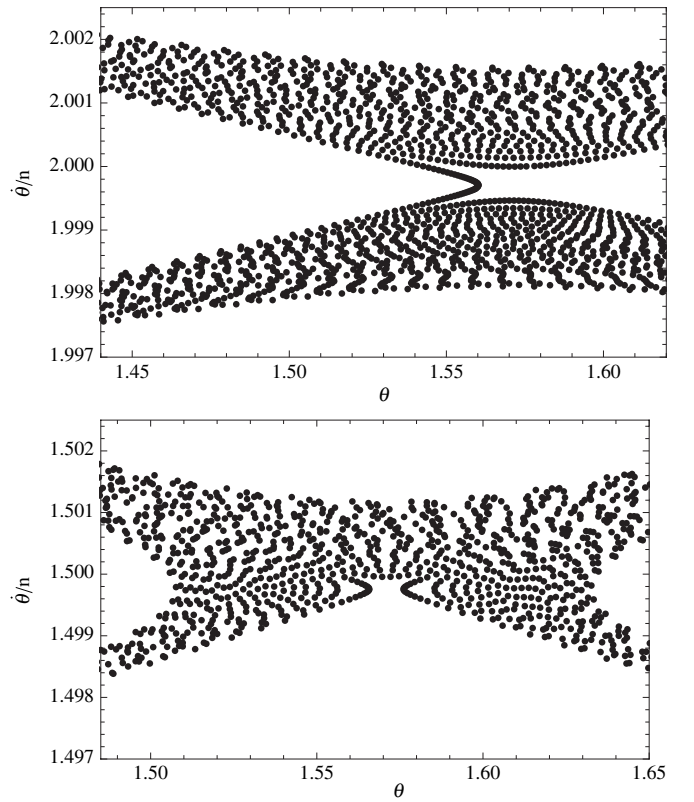


**Figure 7.** Phase space position at times of periastron of a planet passing through 2:1 resonance (top) and captured in 3:2 resonance (bottom).

3:2 resonance capture, respectively. In the case of passage, the trajectory lunges through the opening depicted in Figure 6 from the upper zone of circulation to the lower zone of circulation, reversing its direction. In the case of capture, the trajectory breaches the separatrix between the upper circulation zone and the central zones of pure libration where it follows gradually tightening loops.

The analogy to a rotating pendulum by Goldreich & Peale (1968) can help us to qualitatively understand the alignment required for the planet to traverse resonance. The pendulum is swinging over the top of its support, while a secular torque is slowing down its rotation. Inevitably, the pendulum loses enough rotational energy to be unable to pass the highest point and for a while stops close to the highest point, after which it starts to rotate in the opposite direction, but the secular torque acts in the same direction, this time assisting the pendulum in passing the top in the counterdirection. Once the average $\dot{\gamma}$ changed sign, the pendulum continues to rotate in the counterdirection with acceleration. This also explains why the trajectories in Figure 6 are so flat at the minima of the libration oscillations. Descending step by step to lower spin rates at each libration swing, the trajectories can hardly avoid catching on the nearly linear area of immediate passage through resonance.

This remarkable fact can be further elucidated by analysis of capture probabilities following the lines in Goldreich & Peale (1966). First, we note that the secular tidal torque in the vicinity of a resonance $q'$ (Equation (10)) can be split into two parts, one including the $q = q'$ term and the other the rest of the sum. The $q = q'$ term is an odd function of $\omega_{220q'}$ around zero tidal frequency. The other term, which we call bias, is to a very good approximation constant with $\omega_{220q'}$, because it is the sum of all other secular torques at resonances outside $q'$. These resonances

are spaced by $n$ in $\dot{\gamma} = -\omega_{220q'}$, whereas the amplitude of librations close to a resonance is much smaller (Figures 4 and 5). Figures 1(a) and (b) show that the bias is negative for the given eccentricity, implying a (nearly) frequency-independent dissipation of rotation energy. It is sufficient to consider two librations around the point of resonance $\dot{\gamma} = 0$, i.e., the last libration with positive $\dot{\gamma}$ and the first libration with negative $\dot{\gamma}$. Goldreich & Peale (1966) noted that if the energy offset from zero at the beginning of the last libration above the resonance is uniformly distributed between 0 and $\Delta E = \int \langle T \rangle \dot{\gamma} dt$, where $\langle T \rangle$ is the secular torque, the probability of capture is

$$P_{\text{capt}} = \frac{\delta E}{\Delta E}, \qquad (13)$$

with $\delta E$ being the total change of kinetic energy at the end of the libration below the resonance. Thus, $\langle T \rangle \dot{\gamma}$ should be integrated over one cycle of libration to obtain $\Delta E$, and over two librations symmetric around the resonance $\omega_{220q'} = 0$ to obtain $\delta E$. As a result, the odd part of the tidal torque at $q = q'$ doubles in the integration for $\delta E$, whereas the bias vanishes. For the secular torque in Equation (10), using the singular separatrix solution of zero energy[3]

$$\dot{\gamma} = 2n \left[ \frac{3(B - A)}{C} G_{20q'}(e) \right]^{\frac{1}{2}} \cos \frac{\gamma}{2}, \qquad (14)$$

we obtain

$$P_{\text{capt}} = \frac{2}{1 + 2\pi V / \int_{-\pi}^{\pi} W(\dot{\gamma}) d\gamma} \qquad (15)$$

where

$$V = \sum_q G_{20q}^2(e) K_c(2, |q - q'|n) \, \text{Sign}(q - q')$$

$$W(\dot{\gamma}) = -G_{20q'}^2(e) K_c(2, \dot{\gamma}). \qquad (16)$$

We included the term $q = q'$ for bias $V$ pro forma, because $K_c(2, 0) = 0$. The integral in Equation (15) can be computed numerically using Equation (14). The results of this semi-analytical estimation of capture probability as a function of eccentricity are presented in the top panel of Figure 8. It is gratifying to see that they are in agreement with the results of brute-force simulations discussed in Section 3.1. At $e = 0.205$, the probability of capture in a 3:2 resonance is 1, and the probability of capture in a 2:1 resonance is approximately 0.3.

This fast way of computing capture probabilities can be applied to exoplanets of terrestrial composition, keeping in mind that the probabilities depend on the degree of triaxiality through the parameter $(B - A)/C$ in the equation of separatrix (Equation (14)). Even the smallest exoplanets discovered to date tend to be larger than the Earth because of an observational selection effect. Larger rocky planets are likely to be more axially symmetric. For smaller $(B - A)/C$, keeping all other parameters the same, the curves of capture probabilities in Figure 8 become steeper, so that guaranteed capture is achieved at smaller minimal eccentricities. This is to be expected because if the triaxial torque is turned off in Equation (1), capture is inevitable at any resonance where the tidal torque changes sign. For example, the minimal eccentricities of inevitable capture of a Mercury-like planet with $(B - A)/C = 1.2 \times 10^{-7}$ drop to 0.08 for 3:2, 0.20 for 2:1, and 0.30 for 5:2 resonances.
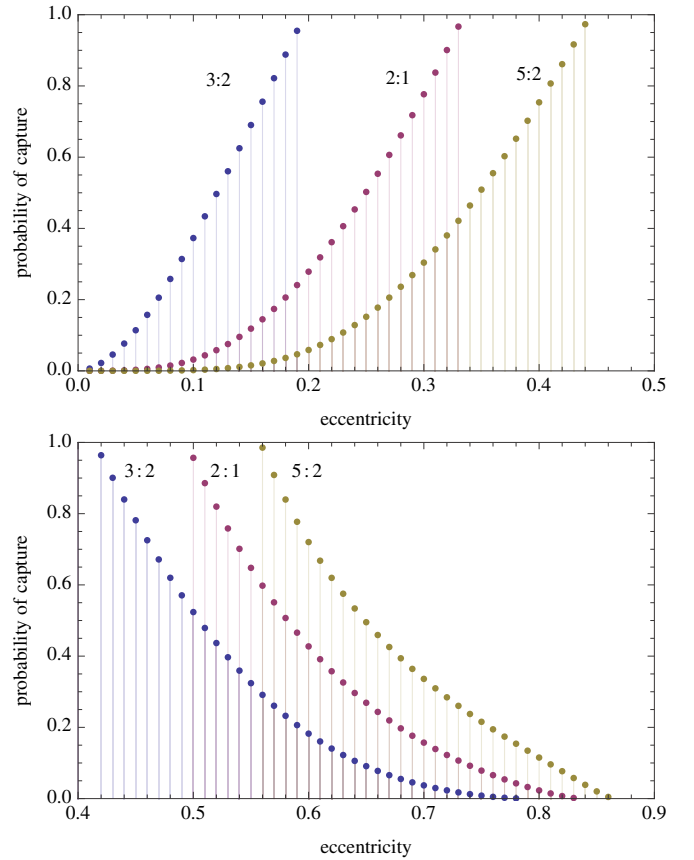
---

[3] Note that our $\gamma$ is twice the $\gamma$ in Goldreich & Peale (1966).



**Figure 8.** Probability of capture of a Mercury-like terrestrial planet in 3:2, 2:1, and 5:2 spin-orbit resonances. Top: prograde evolution when the tidal torque is generally negative and the planet is spun down. Bottom: retrograde evolution when the tidal torque is generally positive and the planet is spun up.

(A color version of this figure is available in the online journal.)

Wieczorek et al. (2011) provided observational evidence that Mercury was previously captured in a synchronous rotation. The authors of this paper explain that this possibility is achievable if the planet started its evolution with a retrograde rotation. The secular tidal torque in this case spins the planet up, first making the rotation prograde, and then driving the planet toward 1:1 resonance. Once captured in synchronous resonance, Mercury could have remained there for an extended period of time, until a fortuitous large impact drove it out of the resonance, abruptly increasing its rate of rotation. Under these circumstances, the planet then could have crossed higher resonances in an upward order. Since the previous consideration of capture probabilities via energy balance is completely symmetric with respect to the direction of $\dot{\gamma}$, Figure 8, top panel, is valid for the reverse crossing of resonances for eccentricities below the equilibrium values. However, more stringent conditions of such retrograde evolution come from the consideration of equilibrium torques in Section 3.2. As follows from Figure 3, a strong impact would not be sufficient for Mercury to leave 1:1 resonance. The orbital eccentricity at the time should be greater than 0.29 to overcome the first barrier of equilibrium torque. Furthermore, the eccentricity should remain above 0.20 for a continuous spin-up to the point of 3:2 resonance. There, Mercury is guaranteed to be captured at any eccentricity between 0.20 and 0.41, because the planet would not be able to spin up any further, whereas the probability of capture at $e > 0.41$ begins to decline with growing eccentricity. Figure 8, bottom panel, shows the probabilities of capture in 3:2, 2:1 and 5:2 resonances for a retrograde

evolution of spin rate, and for eccentricities exceeding the upper limits of the equilibrium torque.[4] Thus, Efroimsky's tidal model described in this paper does not rule out the hypothesis by Wieczorek et al. (2011), but requires, beside the external action, fairly high values of orbital eccentricity during the ascent to the current 3:2 resonance.

The computations presented in this paper for Efroimsky's model of tidal torque serendipitously resolved the long-standing conundrum of Mercury's capture into 3:2 resonance. The previous approximations of tidal torque (Goldreich & Peale 1968; Murray & Dermott 2000) either predicted a low probability of this capture with the current value of eccentricity, or were not able to reproduce the libration damping. Our initial computations imply that the probability of entrapment of Mercury in 3:2 resonance with the current value of eccentricity is 100%. No other outcome would have been possible unless the eccentricity acquired much smaller values in the past, or Mercury's initial rotation was retrograde. A higher eccentricity likely could have resulted in entrapment in 2:1 resonance far in the past when the planet was approaching this rotation rate.

## REFERENCES

Anderson, J. D., Colombo, G., Espsitio, P. B., Lau, E. L., & Trager, G. B. 1987, Icarus, 71, 337
Celletti, A., Froeschlé, C., & Lega, E. 2007, Planet. Space Sci., 55, 889
Correia, A. C. M., & Laskar, J. 2004, Nature, 429, 848
Correia, A. C. M., & Laskar, J. 2009, Icarus, 201, 1
Danby, J. M. A. 1962, Fundamentals of Celestial Mechanics (New York: MacMillan)
Dobrovolskis, A. R. 1995, Icarus, 118, 181
Efroimsky, M. 2012a, ApJ, 746, 150
Efroimsky, M. 2012b, Celest. Mech. Dyn. Astron., 112, 283
Efroimsky, M., & Lainey, V. 2007, J. Geophys. Res., 112, E12003
Efroimsky, M., & Williams, J. G. 2009, Celest. Mech. Dyn. Astron., 104, 257
Ferraz-Mello, S., Rodríguez, A., & Hussmann, H. 2008, Celest. Mech. Dyn. Astron., 101, 171
Goldreich, P., & Peale, S. 1966, AJ, 71, 425
Goldreich, P., & Peale, S. J. 1968, ARA&A, 6, 287
Murray, C. D., & Dermott, S. F. 2000, Solar System Dynamics (Cambridge: Cambridge Univ. Press)
Pettengill, G. H., & Dyce, R. B. 1965, Nature, 206, 1240
Wieczorek, M. A., et al. 2011, Nature Geoscience, 5, 18
Williams, J. G., & Efroimsky, M. 2012, Celest. Mech. Dyn. Astron., submitted

---

[4] Computation of capture probabilities for retrograde evolution by Equation (15) is technically difficult because the Kaula functions vary rapidly at high eccentricities. It is necessary to include more terms in the sum in Equation (10), e.g., $q = -2, -1, \ldots, 8$.